

Detecting topological superconductivity via Berry curvature effects in spectral functions

Yunxiang Liao *

Department of Physics, KTH Royal Institute of Technology, SE-106 91 Stockholm, Sweden

Yi-Ting Hsu †

Department of Physics and Astronomy, University of Notre Dame, South Bend, Indiana 46556, USA



(Received 20 June 2024; revised 1 November 2024; accepted 21 January 2025; published 14 February 2025)

Experimental efforts on topological superconductivity (TSC) have primarily focused on the detection of Majorana boundary modes, while the bulk properties of TSC, particularly in two dimensions, remain relatively underexplored. In this work, we theoretically propose a distinctive signature in the spectral function away from the boundaries, capable of detecting two-dimensional (2D) chiral p -wave TSC induced in a Rashba spin-orbit-coupled heterostructure. This signature can be probed experimentally through angle-resolved photoemission spectroscopy or momentum- and energy-resolved tunneling spectroscopy under a weak magnetic field B . We show that within the topological phase, the spectral intensity of the lowest superconducting band at small momenta $k \sim 0$ brightens (darkens) linearly with increasing B , whereas it darkens (brightens) in the trivial phase when the Rashba system is electron (hole) doped. This sharp contrast arises from the phase-space Berry curvature (BC) of Bogoliubov quasiparticles, a novel quantum geometric property that generalizes the conventional momentum-space BC. The effect of this phase-space BC can also be detected by the differential conductance away from the boundaries. Our falsifiable prediction provides an experimental avenue for detecting Rashba-induced chiral p -wave TSC without relying on Majorana mode detection, addressing a key challenge in the realization of 2D TSC.

DOI: [10.1103/PhysRevB.111.064508](https://doi.org/10.1103/PhysRevB.111.064508)

I. INTRODUCTION

Topological superconductors (TSCs) are exotic quantum materials that exhibit nontrivial band topology in the bulk as well as Majorana modes on different dimensional boundaries [1–7]. The experimental detection of a TSC has remained one of the key challenges in the fields of unconventional superconductivity and topological phases, despite intensive studies in the past decade. Currently, many TSC experiments have focused on detecting Majorana boundary signatures through local scanning probes [3,8–18], although this approach often faces the challenge of distinguishing signals originating from Majorana modes and from other more mundane sources [17–25]. In contrast, experimental features in the bulk of TSC associated with superconducting band topology remain relatively underexplored.

Bands with nontrivial topology necessarily possess nontrivial band geometry, which characterizes the changes in eigenstates at neighboring momenta \mathbf{k} and could have significant influences on experimental observables in metals, insulators, and superconductors [26–37]. Though relatively unexplored, quantum geometric quantities defined in real space and phase space can also lead to detectable experimental features. For example, nontrivial Berry curvature (BC) $\Omega_{\lambda\lambda'}, \lambda, \lambda' = r, k$, is expected for the Bogoliubov

quasiparticles in two-dimensional (2D) chiral TSC, which features a nonzero Chern number $C = \int d\mathbf{k}\Omega_{kk}(\mathbf{k})$ and quantized thermal Hall conductivity [1]. Besides the momentum-space BC, the generalized BCs defined in the real space Ω_{rr} and the phase space Ω_{kr} generally exist in the presence of external perturbations, such as a magnetic field or supercurrent [34]. These generalized BCs were recently found to influence the density of states and thermal responses in spin-singlet superconductors with spin-degenerate normal states [34].

Spin-orbit-coupled (SOC) normal states, on the other hand, have been a crucial ingredient in strategies to achieve TSC since manipulating Fermi surface spin textures can facilitate the formation of effectively spin-triplet Cooper pairs [9,14,15,38–48]. Candidate materials for 2D chiral TSC predicted from this strategy include the proximitized surfaces of topological insulators [38] and hole-doped monolayer transition-metal dichalcogenides [47]. In this work, we will focus on proximitized two-dimensional gas (2DEG) with Rashba SOC [41] [see Fig. 1(a)].

Here, we theoretically predict a BC-induced signature in the spectral function that distinguishes whether the superconducting Rashba 2DEG in Fig. 1(a) is in the topological or trivial phase. This signature is found by examining the generalized BC effects of Bogoliubov quasiparticles using a semiclassical wave-packet analysis [29,34], and can be probed by angular-resolved photoemission spectroscopy (ARPES) or momentum- and energy-resolved tunneling spectroscopy (MERTS) [49] under a weak magnetic field B [50]. We show that the intensity of the lowest superconducting band

*Contact author: liao2@kth.se

†Contact author: yhsu2@nd.edu

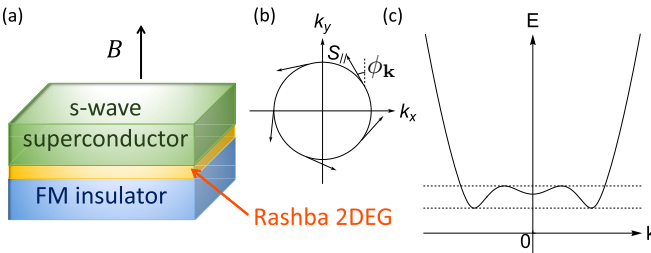


FIG. 1. Sketches for (a) the considered heterostructure hosting an effective 2D TSC, and (b) the in-plane spin texture $S_{||}$ on the Fermi surface of the Rashba layer, where ϕ_k labels the intrinsic locking angle between the spin and momentum. (c) The calculated lower BdG band $E_{-}(k)$ of H , where the dotted lines label the band extrema.

at small momenta $k \sim 0$ brightens (darkens) linearly with B in the topological phase but darkens (brightens) in the trivial phase, when the Rashba 2DEG is electron (hole) doped. This phase-space BC effect can therefore serve as an experimental diagnostic for chiral p -wave TSC realized by a proximitized Rashba 2DEG.

II. MODEL

We consider a well-known minimal model [40,41] that describes the chiral p -wave TSC resulting from a Rashba 2DEG proximitized by a s -wave superconductor and a ferromagnetic insulator (see Fig. 1). In the presence of a weak magnetic field $\mathbf{B} = B\hat{z}$, the 2DEG layer is described by

$$H = \sum_{\sigma=\uparrow,\downarrow} \int d^2\mathbf{r} c_{\sigma}^{\dagger}(\mathbf{r}) \left(\frac{1}{2m} [-i\nabla - \mathbf{A}(\mathbf{r})]^2 - \mu + h\sigma_z \right) c_{\sigma}(\mathbf{r}) + \sum_{\sigma=\uparrow,\downarrow} \int d^2\mathbf{r} c_{\sigma}^{\dagger}(\mathbf{r}) \alpha \{ \sigma \times [-i\nabla - \mathbf{A}(\mathbf{r})] \} \cdot \hat{z} c_{\sigma}(\mathbf{r}) + \int d^2\mathbf{r} (\Delta c_{\uparrow}^{\dagger}(\mathbf{r}) c_{\downarrow}^{\dagger}(\mathbf{r}) + \Delta^* c_{\downarrow}(\mathbf{r}) c_{\uparrow}(\mathbf{r})), \quad (1)$$

where $c_{\sigma}^{\dagger}(\mathbf{r})$ creates an electron at position \mathbf{r} with spin $\sigma = \uparrow, \downarrow$ and mass m , σ_i are spin Pauli matrices, and $\mathbf{A}(\mathbf{r}) = \mathbf{B} \times \mathbf{r}/2$ denotes the vector potential. We have set $\hbar = 1$, the electric charge $e = 1$, and $h > |\mu|$ so that the chemical potential μ intersects only the lower normal band. The second and third lines describe, respectively, the Rashba SOC with strength α and the proximity-induced superconductivity with a pairing potential Δ .

This model is in the chiral p -wave TSC phase when the ferromagnetic exchange coupling $h > \sqrt{|\Delta|^2 + \mu^2}$ and in the trivial phase when $h < \sqrt{|\Delta|^2 + \mu^2}$. In the following calculations, we consider a weak magnetic field $B < |\Delta|$ and a Rashba layer within the TSC or trivial phase. For simplicity, we approximate h and B as two independent variables, assuming that the Zeeman splitting caused by the applied magnetic field and the orbital effect of the ferromagnetic insulator are negligible.

We examine the dynamics of quasiparticles described by H using a semiclassical wave-packet approach, which has been successfully applied to metals [26,29,51] and spin-singlet superconductors with spin-degenerate normal states [32,34,52].

We assume the external perturbation $\mathbf{A}(\mathbf{r})$ is time independent and slowly varying in the real space \mathbf{r} compared to the spread of the wave packet. This allows us to neglect the \mathbf{r} dependence in $\mathbf{A}(\mathbf{r})$ in Eq. (1) and approximating $\mathbf{A}(\mathbf{r})$ by its value at the wave-packet center $\mathbf{r} = \mathbf{r}_c$. Such a scenario can be achieved when the applied field strength is smaller but close to H_{c2} so that the lattice constant of the vortex lattice is close to the coherence length.

The resulting effective Hamiltonian governing the wave-packet dynamics can be further simplified by introducing the Nambu spinor

$$\Psi(\mathbf{k}) = [c_{\uparrow}(\mathbf{k}) \quad c_{\downarrow}(\mathbf{k}) \quad c_{\downarrow}^{\dagger}(-\mathbf{k}) \quad -c_{\uparrow}^{\dagger}(-\mathbf{k})]^T, \quad (2)$$

where

$$c_{\sigma}^{\dagger}(\mathbf{k}) = \int d^2\mathbf{r} e^{i(\mathbf{k} + \mathbf{A}(\mathbf{r}_c)) \cdot \mathbf{r}} c_{\sigma}^{\dagger}(\mathbf{r}). \quad (3)$$

After the transformation, the Hamiltonian assumes the form

$$H = \frac{1}{2} \sum_{\sigma=\uparrow,\downarrow} \int \frac{d^2\mathbf{k}}{(2\pi)^2} \Psi^{\dagger}(\mathbf{k}) h_{\text{BdG}}(\mathbf{k}) \Psi(\mathbf{k}),$$

$$h_{\text{BdG}}(\mathbf{k}) = [\xi_k + \alpha(\sigma_x k_y - \sigma_y k_x)] \tau_z + h \sigma_z + \frac{1}{2} \Delta(\tau_x + i\tau_y) + \frac{1}{2} \Delta^*(\tau_x - i\tau_y). \quad (4)$$

Here $\xi_k = k^2/2m - \mu$ and τ_i denotes the Pauli matrix acting in the Nambu space.

This Hamiltonian can be diagonalized to

$$H = \sum_{s=\pm 1} \int \frac{d^2\mathbf{k}}{(2\pi)^2} E_s(k) \gamma_s^{\dagger}(\mathbf{k}) \gamma_s(\mathbf{k}) + \text{const.}, \quad (5)$$

by applying the Bogoliubov-de Gennes (BdG) transformation:

$$\gamma_s(\mathbf{k}) = \Phi_s^{\dagger}(\mathbf{k}) \Psi(\mathbf{k}), \quad (6)$$

where the helicity $s = \pm$ labels the upper and lower BdG bands. $\Phi_s(\mathbf{k}) = [u_{\uparrow s}(\mathbf{k}) \quad u_{\downarrow s}(\mathbf{k}) \quad v_{\downarrow s}(\mathbf{k}) \quad v_{\uparrow s}(\mathbf{k})]^T$ is the eigenfunction of $h_{\text{BdG}}(\mathbf{k})$ with positive eigenenergy $E_s(k)$ and it satisfies

$$h_{\text{BdG}}(\mathbf{k}) \Phi_s(\mathbf{k}) = E_s(k) \Phi_s(\mathbf{k}). \quad (7)$$

Solving the BdG equation, we find the quasiparticle energy

$$E_s(k) = \left[(\alpha k)^2 + |\Delta|^2 + h^2 + \xi_k^2 + 2s\sqrt{\xi_k^2[(\alpha k)^2 + h^2] + |\Delta|^2 h^2} \right]^{1/2}. \quad (8)$$

For $\xi_k \neq h$ or $s \neq -1$, the BdG eigenfunction $\Phi_s(\mathbf{k})$ is given by,

$$\begin{aligned} u_{\uparrow s}(\mathbf{k}) &= D_s(k) [E_s(k)h\xi_k + |\Delta|^2 h + h\xi_k^2 + \xi_k(\alpha^2 k^2 + h^2) \\ &\quad + s(E_s(k) + h + \xi_k)\sqrt{(\alpha k)^2 \xi_k^2 + h^2(|\Delta|^2 + \xi_k^2)}] \\ &\quad \times e^{i(\chi - \phi_{\mathbf{k}} + \pi/2)/2}, \\ u_{\downarrow s}(\mathbf{k}) &= D_s(k)\alpha k [\xi_k(\xi_k + E_s(k)) \\ &\quad + s\sqrt{(\alpha k)^2 \xi_k^2 + h^2(|\Delta|^2 + \xi_k^2)}] e^{i(\chi + \phi_{\mathbf{k}} - \pi/2)/2}, \\ v_{\downarrow s}(\mathbf{k}) &= D_s(k)|\Delta|[h(h + E_s(k)) \\ &\quad + s\sqrt{(\alpha k)^2 \xi_k^2 + h^2(|\Delta|^2 + \xi_k^2)}] e^{-i(\chi + \phi_{\mathbf{k}} - \pi/2)/2}, \\ v_{\uparrow s}(\mathbf{k}) &= D_s(k)|\Delta|\alpha k(\xi_k - h)e^{-i(\chi - \phi_{\mathbf{k}} + \pi/2)/2}. \end{aligned} \quad (9)$$

By contrast, when $\xi_k = h$ and $s = -1$, we instead have

$$\begin{aligned} u_{\uparrow, -1}(\mathbf{k}) &= 0, \\ u_{\downarrow, -1}(\mathbf{k}) &= D_{-1}(k)|\Delta|e^{i(\chi + \phi_{\mathbf{k}} - \pi/2)/2}, \\ v_{\downarrow, -1}(\mathbf{k}) &= -D_{-1}(k)\alpha k e^{-i(\chi + \phi_{\mathbf{k}} - \pi/2)/2}, \\ v_{\uparrow, -1}(\mathbf{k}) &= D_{-1}(k)E_{-1}(k)e^{-i(\chi - \phi_{\mathbf{k}} + \pi/2)/2}. \end{aligned} \quad (10)$$

Here the phase of the pairing potential $\chi \equiv \arg(\Delta)$ depends on the pairing symmetry [53], the intrinsic angle of the Rashba SOC is denoted by $\phi_{\mathbf{k}} \equiv \arctan(k_y/k_x)$. $D_s(k)$ is the normalization constant.

III. QUASIPARTICLE WAVE PACKET

After diagonalizing H , we construct a wave packet for the quasiparticles from the lower BdG band with $s = -1$:

$$|W_s\rangle = \int_{\mathbf{k}} w_s(\mathbf{k}, t)\gamma_s^\dagger(\mathbf{k})|G\rangle, \quad (11)$$

where $|G\rangle$ denotes the superconducting ground state. The envelope function $w_s(\mathbf{k}, t)$ obeys the normalization condition $\int_{\mathbf{k}} |w_s(\mathbf{k}, t)|^2 = 1$ and is sharply peaked around $\mathbf{k}_c = \int_{\mathbf{k}} |w_s(\mathbf{k}, t)|^2 \mathbf{k}$, whereas the wave-packet center in the real space is given by [32]

$$\mathbf{r}_c = i \int_{\mathbf{k}} (w_s(\mathbf{k}, t)\Phi_s(\mathbf{k}))^\dagger \partial_{\mathbf{k}} (w_s(\mathbf{k}, t)\Phi_s(\mathbf{k})). \quad (12)$$

For cases where the perturbation is strong, a treatment involving both $s = \pm$ bands is required [28,29,54], which falls beyond the scope of our current study.

The semiclassical dynamics of this quasiparticle wave packet $|W_s\rangle$ is described by its Lagrangian L , given by the wave-packet average [55] of the operator $\hat{L} = i \frac{d}{dt} - \hat{H}$ [29,34]. It can be expressed in terms of the momentum-space and real-space Berry connections \mathcal{A}_{ks} and \mathcal{A}_{rs} as

$$L = -E_s(k_c) - \dot{\mathbf{k}}_c \cdot \mathbf{r}_c + \dot{\mathbf{k}}_c \cdot \mathcal{A}_{ks} + \dot{\mathbf{r}}_c \cdot \mathcal{A}_{rs}. \quad (13)$$

The momentum-space Berry connection \mathcal{A}_{ks} is defined in terms of the BdG wavefunction $\Phi_s(\mathbf{k})$ as $\mathcal{A}_{ks} = i\Phi_s^\dagger(\mathbf{k}_c)\partial_{\mathbf{k}_c}\Phi_s(\mathbf{k}_c)$, and can be further simplified into

$$\mathcal{A}_{ks} = -\frac{1}{2}\rho_{0s}(\mathbf{k}_c)\partial_{\mathbf{k}_c}\chi + \frac{1}{2}\rho_{1s}(\mathbf{k}_c)\partial_{\mathbf{k}_c}\phi_{\mathbf{k}_c}. \quad (14)$$

Here

$$\rho_{as}(\mathbf{k}) = \sum_{\sigma} (\zeta_{\sigma})^a (|u_{\sigma s}(\mathbf{k})|^2 - |v_{\sigma s}(\mathbf{k})|^2) \quad (15)$$

with $a = 0, 1$ and $\zeta_{\uparrow/\downarrow} = \pm 1$. Physically speaking, $\rho_{0s}(\mathbf{k}_c)$ and $\rho_{1s}(\mathbf{k}_c)/2$ correspond to the wave-packet average [55] of the total charge and spin, respectively (see Appendix A).

The real-space Berry connection \mathcal{A}_{rs} is given by

$$\mathcal{A}_{rs} = \tilde{\mathcal{A}}_{rs} + \rho_{0s}(\mathbf{k}_c)\mathbf{A}(\mathbf{r}_c) + \frac{1}{2}\mathbf{B} \times \mathbf{d}, \quad (16)$$

where $\tilde{\mathcal{A}}_{rs}$ is the real-space analog of \mathcal{A}_{ks} in Eq. (14) by replacing $\partial_{\mathbf{k}_c} \rightarrow \partial_{\mathbf{r}_c}$. The second term describes how the total charge of the wave packet $\rho_{0s}(\mathbf{k}_c)$ couples to the external vector potential $\mathbf{A}(\mathbf{r}_c)$, whereas the last term describes how the charge dipole moment \mathbf{d} of the wave packet couples to the external magnetic field \mathbf{B} . Note that these two terms enter the Lagrangian in Eq. (13) in the same way as the well-known Lagrangian describing the Lorentz force of a charged object with a dipole moment in a magnetic field [56].

The dipole moment \mathbf{d} of the wave packet, given by the wave-packet average [55] of dipole moment operator $\hat{\mathbf{d}} = \sum_{\sigma} \int d^2\mathbf{r} \hat{c}_{\sigma}^\dagger(\mathbf{r})\hat{c}_{\sigma}(\mathbf{r})(\mathbf{r} - \mathbf{r}_c)$, contains two terms $\mathbf{d} = \mathbf{d}_1 + \mathbf{d}_2$. The first term

$$\mathbf{d}_1 = \frac{1}{2}(\rho_{0s}^2(\mathbf{k}_c) - 1)\partial_{\mathbf{k}_c}\chi, \quad (17)$$

was found nonzero for a d -wave pairing potential [34], but vanishes for our case of an s -wave pairing potential with $\partial_{\mathbf{k}}\chi = 0$. Nonetheless, we find that the second term

$$\mathbf{d}_2 = \frac{1}{2}[\rho_{2s}(\mathbf{k}_c) - \rho_{0s}(\mathbf{k}_c)\rho_{1s}(\mathbf{k}_c)]\partial_{\mathbf{k}_c}\phi_{\mathbf{k}_c}, \quad (18)$$

is a new source of dipole moment arising from the SOC. Note that although \mathbf{d}_2 scales with the winding of the Rashba angle $\phi_{\mathbf{k}_c}$ (Fig. 1), it is not inherited from the normal state because the prefactor $\rho_{2s} - \rho_{0s}\rho_{1s} = 0$ when the pairing potential $\Delta = 0$, where

$$\rho_{2s}(\mathbf{k}_c) = \sum_{\sigma} \zeta_{\sigma} (|u_{\sigma s}(\mathbf{k}_c)|^2 + |v_{\sigma s}(\mathbf{k}_c)|^2). \quad (19)$$

Thus, \mathbf{d}_2 exists only in the superconducting state but not the normal state.

This is physically because the quasiparticle wave packet consists of momentum- and position-dependent mixtures of electron and hole components, which allows a deviation of the wave-packet center \mathbf{r}_c from the charge center. Since the dipole moment \mathbf{d}_2 emerges exclusively when superconductivity and spin-orbit coupling coexist, \mathbf{d}_2 can lead to new experimental features of SOC superconductors through coupling to an external \mathbf{B} field [see Eq. (6)].

IV. PHASE-SPACE BC AND DENSITY OF STATES

To analyze the experimental features of \mathbf{d}_2 -induced BC, we examine how the wave-packet dynamics are modified by BC from Eq. (13):

$$\begin{bmatrix} \Omega_{rrs}^{ij} & \Omega_{rks}^{ij} - \delta_{ij} \\ \Omega_{krs}^{ij} + \delta_{ij} & \Omega_{kks}^{ij} \end{bmatrix} \begin{bmatrix} \dot{\mathbf{r}}_c^j \\ \dot{\mathbf{k}}_c^j \end{bmatrix} = \begin{bmatrix} \partial_{r_i} E_s(k_c) \\ \partial_{k_i} E_s(k_c) \end{bmatrix}, \quad (20)$$

where the repeated Cartesian indices are implicitly summed. The momentum-, real-, and phase-space BCs are defined as

the derivatives of the Berry connections \mathcal{A}_{rs} and \mathcal{A}_{ks} :

$$\Omega_{\lambda\lambda's}^{ij} \equiv \partial_{\lambda'c} \mathcal{A}_{\lambda's}^j - \partial_{\lambda'c} \mathcal{A}_{\lambda's}^i, \quad \lambda, \lambda' = r, k. \quad (21)$$

For the $p + ip$ TSC we consider in Eq. (1), we find that the momentum- and phase-space BC under an external \mathbf{B} field are given by (see Appendix C)

$$\Omega_{ks} = \frac{1}{2} \partial_{\mathbf{k}_c} \rho_{1s}(\mathbf{k}_c) \times \partial_{\mathbf{k}_c} \phi_{\mathbf{k}_c}, \quad \Omega_{rks}^{ij} = -\frac{1}{2} \partial_{k_c^i} (\mathbf{B} \times \mathbf{d})^j, \quad (22)$$

up to the leading order in the real-space gradient expansion, where field-induced supercurrent is not considered in this work. We find that while the presence of real-space BC $\Omega_{rs} = \rho_{0s}(\mathbf{k}_c) \mathbf{B}$ does not depend on SOC, neither Ω_{ks} nor Ω_{rks}^{ij} would have survived in the absence of the SOC. Specifically, the momentum-space Ω_{ks} is inherited from the spin-orbit coupled normal state, whereas the phase-space Ω_{rks} describes the coupling between the SOC-induced wave-packet dipole moment to the external \mathbf{B} field.

The BC effects on the semiclassical dynamics in Eq. (20) have been shown [27,29] to modify the phase-space density of states $D(\mathbf{r}, \mathbf{k})$, required by the conservation of the total number of states $\mathcal{N} = D(\mathbf{r}, \mathbf{k}) \Delta V$ in a phase-space volume $\Delta V = \Delta k \Delta r$ (see Appendix D). The modified phase-space density of states was shown to be [29,34,57] $D(\mathbf{r}, \mathbf{k}) \approx 1 + \text{Tr} \Omega_{rks} - \Omega_{rs} \cdot \Omega_{ks}$ up to an inessential overall coefficient, where a spatial gradient expansion is applied for slowly varying external fields. This BC-modified phase-space density of states $D(\mathbf{r}, \mathbf{k})$ is the key factor that embeds the information of the wave-packet BCs we find in Eq. (22) into experimental observables.

For the $p + ip$ TSC we consider, we obtain the BC-induced phase-space density of states $\delta D = D - 1$ under an external \mathbf{B} field using Eq. (22)

$$\delta D = -\frac{1}{2} \mathbf{B} \cdot (\nabla_{\mathbf{k}} \times \mathbf{d}_2) - \frac{1}{2} (\rho_{0s} \nabla_{\mathbf{k}} \rho_{1s} \times \nabla_{\mathbf{k}} \phi_{\mathbf{k}}) \cdot \mathbf{B} \quad (23)$$

up to the leading order in spatial gradient $\partial_{\mathbf{r}}$. Note that δD exists only in the presence of SOC: The latter term results from the momentum- and real-space BC, which is proportional to the winding of the Rashba angle $\phi_{\mathbf{k}}$ in the spin-orbit-coupled normal state. The former term results from the phase-space BC, which exists only in a spin-orbit-coupled superconductor due to the quasiparticle charge dipole moment \mathbf{d}_2 in Eq. (7).

V. BC-INDUCED TOPOLOGICAL SIGNATURES IN OBSERVABLES

We are now ready to examine how the BCs influence the experimental observables in a $p + ip$ TSC enabled by Rashba SOC. With the BC-modified phase-space density of states $D = 1 + \delta D$, we investigate the spectral function $A(\mathbf{k}, \omega)$ and the normal metal-to-superconductor tunneling conductance [58] $G(\mathbf{r}, \omega)$ given by

$$A(\mathbf{k}, \omega) = \sum_{\sigma} \int_{\mathbf{r}} D(\mathbf{r}, \mathbf{k}) [|u_{\sigma s}(\mathbf{k})|^2 \delta(\omega - E_s(k)) + |v_{\sigma s}(\mathbf{k})|^2 \delta(\omega + E_s(k))], \quad (24a)$$

$$G(\mathbf{r}, \omega) = \sum_{\sigma} \int_{\mathbf{k}} D(\mathbf{r}, \mathbf{k}) [|u_{\sigma s}(\mathbf{k})|^2 \delta(\omega - E_s(k)) + |v_{\sigma s}(\mathbf{k})|^2 \delta(\omega + E_s(k))], \quad (24b)$$

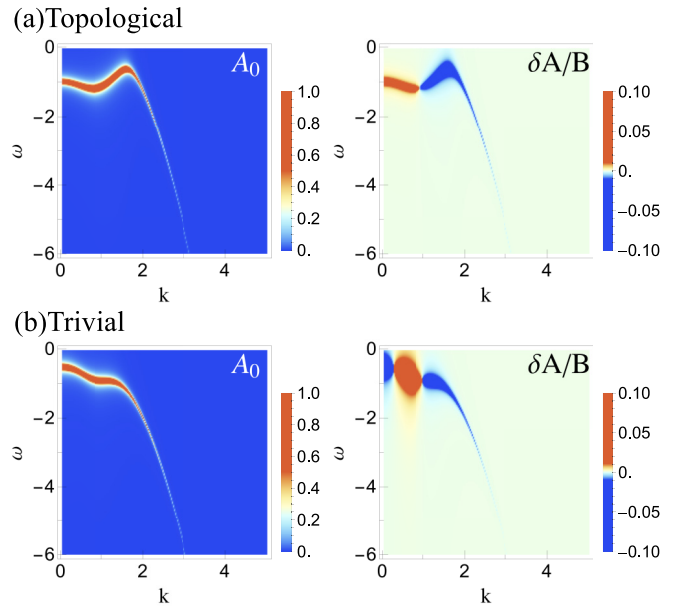


FIG. 2. BC effects on the spectral function $A(\mathbf{k}, \omega)$ in the (a) topological phase and (b) trivial phase. The bare spectral function $A_0(\mathbf{k}, \omega)$ and the BC contribution per unit field strength $\delta A(\mathbf{k}, \omega)/B$ are shown on the left and right panels, respectively. Here, we set $h = 2$ and $h = 0.5$ in (a) and (b), respectively, whereas we fix the pairing potential $\Delta = 1$, chemical potential $\mu = 0.2$, mass $m = 0.5$, and SOC strength $\alpha = 1$ in all figures unless specified otherwise. This figure and Fig. 4 are generated by replacing the Dirac delta function in Eq. (24) with a Lorentzian $L(\omega) = \frac{1}{\pi} \frac{\eta/2}{\omega^2 + (\eta/2)^2}$ of width $\eta = 0.05$.

where we focus on the lower BdG band $s = -$ and neglect the small spatial variations in $D(\mathbf{r}, \mathbf{k})$ given the slowly varying perturbation. The spectral function can be probed by the momentum- and energy-resolved tunneling spectroscopy MERTS [49] or in principle ARPES under a weak magnetic field. The tunneling conductance can be measured by STM or tunneling junctions. For STM measurements that require access to open surfaces, a bilayer structure [15] could be more feasible than the heterostructure in Fig. 1(a).

First, we demonstrate the BC effects in the spectral function $A = A_0 + \delta A$ in Fig. 2. The uncorrected spectral function $A_0(\mathbf{k}, \omega)$ and the BC contribution $\delta A(\mathbf{k}, \omega)$ are obtained by setting $D(\mathbf{k}) = 1$ and $\delta D(\mathbf{k})$ in Eq. (24a), respectively. At zero field $\mathbf{B} = 0$, the magnitude of A_0 reaches its peaks at frequencies along the lower superconducting band $\omega = -E_{-}(\mathbf{k})$ [see Fig. 2(a)]. Under an applied field B , the BC contribution δA is activated, which modulates the peak intensities in A_0 in a momentum-dependent way tied to topology: In the topological phase where $h > \sqrt{\Delta^2 + \mu^2}$, the peak intensity at small momenta $\mathbf{k} \sim 0$ is enhanced by $\delta A > 0$, as shown in Fig. 2(a). In contrast, in the topologically trivial phase where $h < \sqrt{\Delta^2 + \mu^2}$, we find a suppression $\delta A < 0$ at $\mathbf{k} \sim 0$, as shown in Fig. 2(b). In either phase, the magnitude of BC-induced enhancement or suppression $|\delta A|$ increases linearly with B until it reaches the critical field strength.

Now, we show how the topological conditions explicitly enter the BC-modified spectral function $A = A_0 + \delta A$ at $\mathbf{k} = 0$. For superconductivity described by the model H in Eq. (1),

the topological conditions refer to (1) the Rashba strength $\alpha \neq 0$ is nonzero and (2) $h^2 > (\Delta^2 + \mu^2)$. To link these two conditions to the BC effect in the spectral function, we insert the full expressions of the coherence factors $u_{\sigma s}(\mathbf{k}_c)$ and $v_{\sigma s}(\mathbf{k}_c)$ into the BC-induced change $\delta D(\mathbf{k})$ in the phase-space density of states [see Eq. (23)] and arrive at

$$\delta D(k=0) = B\alpha^2 \frac{\mu(h\Delta^2 + (h^2 - \mu^2)\sqrt{\Delta^2 + \mu^2})}{2h^2(\Delta^2 + \mu^2)(h^2 - \Delta^2 - \mu^2)}. \quad (25)$$

It is clear from Eq. (25) that when only the lower normal band involves in pairing $h > |\mu|$, criterion (1) and (2) indicate that the BC-induced change $\delta D(k=0)$ takes the sign of the chemical potential μ in the topological phase and its opposite in the trivial phase, respectively. Together with the fact that the normalized BC contribution $\delta A(\mathbf{k}, \omega)/A_0(\mathbf{k}, \omega) = \delta D(\mathbf{k}, \omega)$ at $\omega = -E_-(\mathbf{k})$, which follows from Eq. (24a), we conclude that the sign of the BC effect δA at momentum $\mathbf{k} = 0$ qualitatively detects whether the superconductivity is in the topological or trivial phases.

Experimentally, this topological signature can be detected in the following way: First, determine whether the chemical potential of the 2DEG is $\mu > 0$ or $\mu < 0$, i.e., whether μ is closer to the higher or lower band bottom. Then in the former (latter) case, one can identify whether the 2D superconductivity is in the topological (trivial) or trivial (topological) phase if the ARPES or MERTS signal intensity enhances $\delta A > 0$ or suppresses $\delta A \leq 0$ when an applied weak magnetic field is applied. This change in intensity δA is expected to grow linearly with the field strength B [59].

Moreover, this topological signature can be amplified quadratically by the Rashba SOC strength α since Eq. (25) indicates that $\delta A/A_0 = \delta D \propto \alpha^2$ at $k = 0$. We demonstrate this drastic change in α at small momenta in Figs. 3(a) and 3(b) in the topological and trivial phases, respectively, along with the bare spectral function $A_0(\mathbf{k}, \omega)$ for the lower superconducting band $\omega = -E_-(\mathbf{k})$. In contrast to the small momenta regime, the large momenta regime does not show clear monotonic dependence in α . Besides amplifying the topological signature, this α^2 enhancement at $k = 0$ can be used to quantitatively determine the relative SOC strength between two different Rashba layers or interfaces within otherwise identical heterostructures.

In contrast to the spectral function, the BC-modified tunneling conductance $G(\omega) = G_0(\omega) + \delta G(\omega)$ is not an effective topological diagnostic. We contrast the results in the topological and trivial phases in Fig. 4, where we omit the position dependence since the signal is nearly uniform at the scale of the wave packet. Here, the bare conductance G_0 and the BC correction δG are plotted using Eq. (24b) by taking $D(\mathbf{k})$ to be 1 and $\delta D(\mathbf{k})$, respectively. The bare conductance G_0 shows four coherence peaks at frequencies ω marked by dotted lines, where the peak intensities are not particle-hole symmetric since the effective pairing symmetry is not s wave [58]. These peaks originate from the band extrema of the lower BdG band [see Fig. 1(c)], which are accessible in the low-density regime. In experiments, the number of visible coherence peaks is determined by the normal state band structure, thermal and impurity-caused smearing, and the focused

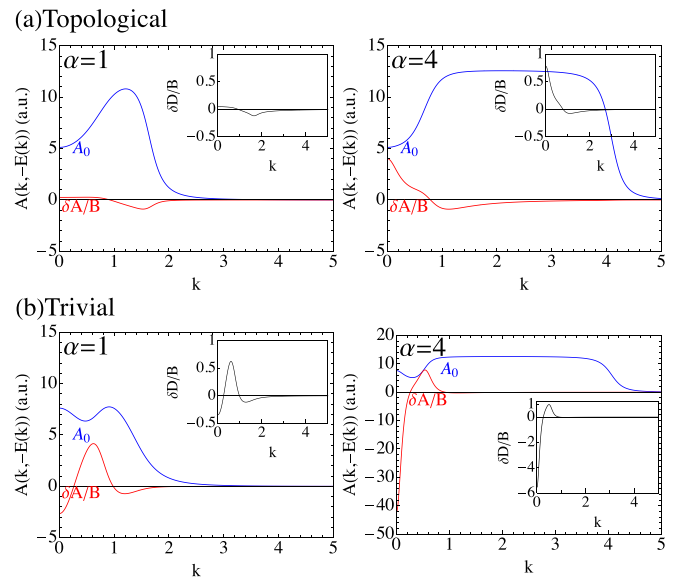


FIG. 3. The bare spectral functions $A_0(\mathbf{k}, \omega)$ and BC contribution per field strength $\delta A/B$ at weak (left) and strong (right) SOC strength α in the (a) topological and (b) trivial phases. The spectral functions are plotted along the lower superconducting band $\omega = -E_-(\mathbf{k})$ at each momentum \mathbf{k} . The exchange coupling is set to $h = 2$ and $h = 0.5$ in (a) and (b), whereas the SOC strength is set to $\alpha = 1$ and $\alpha = 4$ in the left and right panels, respectively. Note that the normalized BC contribution to the spectral function $\frac{\delta A/B}{A_0}$ is directly given by the BC contribution to phase-space DOS per field strength $\delta D/B$, as shown in the insets.

frequency range. The bare signal G_0 with no BC effect is given by the tunneling spectrum at zero field $\mathbf{B} = 0$.

When a weak magnetic field \mathbf{B} is applied, the BC contribution δG considerably suppresses the strengths of the two lower-energy coherence peaks but not the higher-energy peaks in Fig. 4(a). As we tune the strengths of the exchange coupling h and SOC α within the topological regime, we generally find a peak suppression or/and enhancement in intensities that are nonuniform in frequency ω and grows linearly with an applied field B weaker than the critical field. Nonetheless, the information about the topological conditions in Eq. (25)

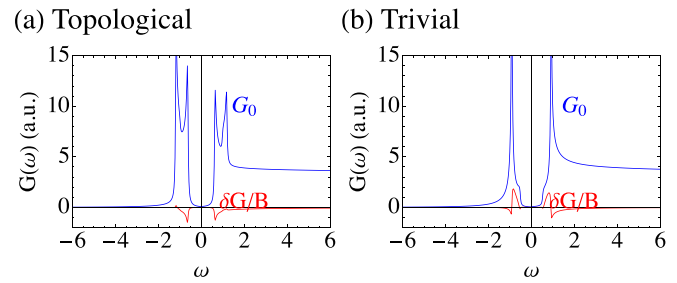


FIG. 4. The BC effects in the tunneling conductance $G(\omega)$ in the (a) topological phase $h = 2$ and (b) the trivial case with $h = 0.5$. The blue curves G_0 are the bare tunneling conductance obtained with $D(\mathbf{k}) = 1$, i.e., at $B = 0$. The red curves $\delta G/B$ are the corrections per unit magnetic field B to G_0 from the BC-induced change in the phase-space DOS, calculated from Eq. (24) with $D(\mathbf{k})$ replaced by $\delta D(\mathbf{k})$. We set the SOC strength to be $\alpha = 1$ as in Fig 2.

becomes convoluted in $G(\omega)$ due to the momentum integral in Eq. (24b). Therefore, the distinction between the BC effects in the topological and trivial phases seems quantitative or qualitative in a complicated way [see Fig. 4(b)]. Despite that the distinction is quantitative in $G(\omega)$ between topological and trivial phases, our analyses point out that one should expect such B-field-activated nonuniform modulation in experiments due to the phase-space BC. Such BC effect is most easily detectable in lightly doped TSC candidate materials where multiple coherence peaks are visible.

ACKNOWLEDGMENTS

Y.L. and Y.-T.H. are grateful for the very helpful discussions with Jay Sau. Y.-T.H. also acknowledges helpful discussion with Jhih-Shih You at the initial stage of the project. Y.L. acknowledges support from a postdoctoral fellowship from the Simons Foundation “Ultra-Quantum Matter” Research Collaboration. Y.-T.H. acknowledges support from Department of Energy Basic Energy Science Award No. DE-SC0024291. Y.-T.H. acknowledges support from NSF Grant No. DMR-2238748. This work was performed in part at Aspen Center for Physics, which is supported by National Science Foundation Grant No. PHY-2210452. This work was supported in part by the National Science Foundation under Grant No. NSF PHY-1748958.

APPENDIX A: WAVE-PACKET PROPERTIES

In this Appendix, we derive some of the key properties of quasiparticle wave packet discussed in the main text. The wave-packet center coordinate in the real space defined in Eq. (12) [32] can be expressed in terms of the coherence factors as

$$\mathbf{r}_c = \partial_{\mathbf{k}_c} \theta_w(\mathbf{k}_c, t) + i \sum_{\sigma} (u_{\sigma s}^*(\mathbf{k}_c) \partial_{\mathbf{k}_c} u_{\sigma s}(\mathbf{k}_c) + v_{\sigma s}^*(\mathbf{k}_c) \partial_{\mathbf{k}_c} v_{\sigma s}(\mathbf{k}_c)). \quad (\text{A1})$$

we find

$$\begin{aligned} \langle W_s | \gamma_{s_1}^\dagger(\mathbf{k}_1) \gamma_{s_2}(\mathbf{k}_2) | W_s \rangle &= \int_{\mathbf{k}'_1, \mathbf{k}'_2} w_s^*(\mathbf{k}'_1, t) w_s(\mathbf{k}'_2, t) \langle G | \gamma_s(\mathbf{k}'_1) \gamma_{s_1}^\dagger(\mathbf{k}_1) \gamma_{s_2}(\mathbf{k}_2) \gamma_s^\dagger(\mathbf{k}'_2) | G \rangle \\ &= w_s^*(\mathbf{k}_1, t) w_s(\mathbf{k}_2, t) \delta_{s, s_2} \delta_{s, s_1}, \\ \langle W_s | \gamma_{s_1}(\mathbf{k}_1) \gamma_{s_2}^\dagger(\mathbf{k}_2) | W_s \rangle &= \int_{\mathbf{k}'_1, \mathbf{k}'_2} w_s^*(\mathbf{k}'_1, t) w_s(\mathbf{k}'_2, t) \langle G | \gamma_s(\mathbf{k}'_1) \gamma_{s_1}(\mathbf{k}_1) \gamma_{s_2}^\dagger(\mathbf{k}_2) \gamma_s^\dagger(\mathbf{k}'_2) | G \rangle \\ &= \delta_{\mathbf{k}_1, \mathbf{k}_2} \delta_{s_1, s_2} - \delta_{s, s_1} \delta_{s, s_2} w_s^*(\mathbf{k}_2, t) w_s(\mathbf{k}_1, t) \end{aligned} \quad (\text{A7})$$

For $\hat{O} = \hat{Q}$ or \hat{S} , it is easy to see that the equation above can be further simplified to

$$\begin{aligned} Q &= \int_{\mathbf{k}} |w_s(\mathbf{k}, t)|^2 \rho_{0s}(\mathbf{k}) = \rho_{0s}(\mathbf{k}_c), \\ S &= \frac{1}{2} \int_{\mathbf{k}} |w_s(\mathbf{k}, t)|^2 \rho_{1s}(\mathbf{k}) = \frac{1}{2} \rho_{1s}(\mathbf{k}_c). \end{aligned} \quad (\text{A9})$$

For the charge dipole moment \mathbf{d} , one can express $\mathbf{r}e^{-i(\mathbf{k}_1-\mathbf{k}_2)\cdot\mathbf{r}}$ in the Eq. (A8) as $-i\partial_{\mathbf{k}_2}e^{-i(\mathbf{k}_1-\mathbf{k}_2)\cdot\mathbf{r}}$, which results in

$$\begin{aligned}
 \langle W_s | \hat{\mathbf{d}} | W_s \rangle - \langle G | \hat{\mathbf{d}} | G \rangle &= \sum_{\sigma} \int_{\mathbf{r}} \int_{\mathbf{k}_1, \mathbf{k}_2} (-i\partial_{\mathbf{k}_2}e^{-i(\mathbf{k}_1-\mathbf{k}_2)\cdot\mathbf{r}}) w_s^*(\mathbf{k}_1, t) w_s(\mathbf{k}_2, t) [u_{\sigma s}^*(\mathbf{k}_1) u_{\sigma s}(\mathbf{k}_2) - v_{\sigma s}^*(\mathbf{k}_1) v_{\sigma s}(\mathbf{k}_2)] - \mathbf{r}_c Q \\
 &= i \sum_{\sigma} \int_{\mathbf{k}} w_s^*(\mathbf{k}, t) (\partial_{\mathbf{k}} w_s(\mathbf{k}, t)) (|u_{\sigma s}(\mathbf{k})|^2 - |v_{\sigma s}(\mathbf{k})|^2) + i \sum_{\sigma} \int_{\mathbf{k}} |w_s(\mathbf{k}, t)|^2 (u_{\sigma s}^*(\mathbf{k}) \partial_{\mathbf{k}} u_{\sigma s}(\mathbf{k}) \\
 &\quad - v_{\sigma s}^*(\mathbf{k}) \partial_{\mathbf{k}} v_{\sigma s}(\mathbf{k})) - \mathbf{r}_c Q \\
 &= \int_{\mathbf{k}} |w_s(\mathbf{k}, t)|^2 (\rho_{0s}(\mathbf{k}) \partial_{\mathbf{k}} \theta_w(\mathbf{k}, t) - \partial_{\mathbf{k}} \chi/2 + \rho_{2s}(\mathbf{k}) \partial_{\mathbf{k}} \phi_{\mathbf{k}}/2) - \mathbf{r}_c Q \\
 &\quad + \frac{i}{2} \sum_{\sigma} \int_{\mathbf{k}} (\partial_{\mathbf{k}} |w_s(\mathbf{k}, t)|^2) (|u_{\sigma s}(\mathbf{k})|^2 - |v_{\sigma s}(\mathbf{k})|^2) + \frac{i}{2} \sum_{\sigma} \int_{\mathbf{k}} |w_s(\mathbf{k}, t)|^2 \partial_{\mathbf{k}} (|u_{\sigma s}(\mathbf{k})|^2 - |v_{\sigma s}(\mathbf{k})|^2) \\
 &= \rho_{0s}(\mathbf{k}_c) \partial_{\mathbf{k}_c} \theta_w(\mathbf{k}_c, t) - \partial_{\mathbf{k}_c} \chi/2 + \rho_{2s}(\mathbf{k}_c) \partial_{\mathbf{k}_c} \phi_{\mathbf{k}_c}/2 - \mathbf{r}_c \rho_{0s}(\mathbf{k}_c). \tag{A10}
 \end{aligned}$$

Inserting the expression for \mathbf{r}_c in Eq. (A3), we find the wave-packet average of the charge dipole moment is given by

$$\mathbf{d} = \frac{1}{2} (\rho_{0s}^2(\mathbf{k}_c) - 1) \partial_{\mathbf{k}_c} \chi + \frac{1}{2} (\rho_{2s}(\mathbf{k}_c) - \rho_{0s}(\mathbf{k}_c) \rho_{1s}(\mathbf{k}_c)) \partial_{\mathbf{k}_c} \phi_{\mathbf{k}_c}, \tag{A11}$$

where the first and second terms correspond to \mathbf{d}_1 in Eq. (17) and \mathbf{d}_2 in Eq. (18), respectively.

APPENDIX B: LAGRANGIAN

This Appendix evaluates the Lagrangian which governs the semiclassical dynamics of the wave packet:

$$L = \langle W_s | \left(i \frac{d}{dt} - H \right) | W_s \rangle - \langle G | \left(i \frac{d}{dt} - H \right) | G \rangle. \tag{B1}$$

The part that contains the Hamiltonian is given by

$$\begin{aligned}
 \langle W_s | H | W_s \rangle - \langle G | H | G \rangle &= \int_{\mathbf{k}_1, \mathbf{k}_2} w_s^*(\mathbf{k}_1, t) w_s(\mathbf{k}_2, t) \langle G | \gamma_s(\mathbf{k}_1) \left(\int_{\mathbf{k}} \sum_{s'} E_{s'}(k) \gamma_{s'}^\dagger(\mathbf{k}) \gamma_{s'}(\mathbf{k}) \right) \gamma_s^\dagger(\mathbf{k}_2) | G \rangle \\
 &= \int_{\mathbf{k}} |w_s(\mathbf{k}, t)|^2 E_s(k) = E_s(k_c), \tag{B2}
 \end{aligned}$$

while the part that involves the time derivative reduces to

$$\begin{aligned}
 \langle W_s | i \frac{d}{dt} | W_s \rangle &= i \int_{\mathbf{k}} w_s^*(\mathbf{k}, t) \frac{\partial}{\partial t} w_s(\mathbf{k}, t) + i \frac{d\mathbf{r}_c}{dt} \cdot \int_{\mathbf{k}} w_s^*(\mathbf{k}, t) \frac{\partial}{\partial \mathbf{r}_c} w_s(\mathbf{k}, t) \\
 &\quad + i \frac{d\mathbf{r}_c}{dt} \cdot \int_{\mathbf{k}_1, \mathbf{k}_2} w_s^*(\mathbf{k}_1, t) w_s(\mathbf{k}_2, t) \langle G | \gamma_s(\mathbf{k}_1) \left(\frac{\partial}{\partial \mathbf{r}_c} \gamma_s^\dagger(\mathbf{k}_2) \right) | G \rangle. \tag{B3}
 \end{aligned}$$

Note that the time dependence of the quasiparticle creation operator γ_s^\dagger comes from the time dependence of the wave-packet center \mathbf{r}_c .

Using the BdG transformation Eq. (6), the term $\langle W_s | i \frac{d}{dt} | W_s \rangle$ can be further divided into three parts:

$$\begin{aligned}
 \langle W_s | i \frac{d}{dt} | W_s \rangle &= L_1 + L_2 + L_3, \\
 L_1 &= i \int_{\mathbf{k}} w_s^*(\mathbf{k}, t) \frac{\partial}{\partial t} w_s(\mathbf{k}, t) + i \frac{d\mathbf{r}_c}{dt} \cdot \int_{\mathbf{k}} w_s^*(\mathbf{k}, t) \frac{\partial}{\partial \mathbf{r}_c} w_s(\mathbf{k}, t) \\
 L_2 &= i \frac{d\mathbf{r}_c}{dt} \cdot \int_{\mathbf{k}_1, \mathbf{k}_2} w_s^*(\mathbf{k}_1, t) w_s(\mathbf{k}_2, t) \\
 &\quad \times \langle G | \gamma_s(\mathbf{k}_1) \left[\left(\frac{\partial}{\partial \mathbf{r}_c} u_{\uparrow s}(\mathbf{k}_2) \right) c_{\uparrow}^\dagger(\mathbf{k}_2) + \left(\frac{\partial}{\partial \mathbf{r}_c} u_{\downarrow s}(\mathbf{k}_2) \right) c_{\downarrow}^\dagger(\mathbf{k}_2) + \left(\frac{\partial}{\partial \mathbf{r}_c} v_{\downarrow s}(\mathbf{k}_2) \right) c_{\downarrow}(-\mathbf{k}_2) - \left(\frac{\partial}{\partial \mathbf{r}_c} v_{\uparrow s}(\mathbf{k}_2) \right) c_{\uparrow}(-\mathbf{k}_2) \right] | G \rangle, \\
 L_3 &= i \frac{d\mathbf{r}_c}{dt} \cdot \int_{\mathbf{k}_1, \mathbf{k}_2} w_s^*(\mathbf{k}_1, t) w_s(\mathbf{k}_2, t) \\
 &\quad \times \langle G | \gamma_s(\mathbf{k}_1) \left[u_{\uparrow s}(\mathbf{k}_2) \left(\frac{\partial}{\partial \mathbf{r}_c} c_{\uparrow}^\dagger(\mathbf{k}_2) \right) + u_{\downarrow s}(\mathbf{k}_2) \left(\frac{\partial}{\partial \mathbf{r}_c} c_{\downarrow}^\dagger(\mathbf{k}_2) \right) + v_{\downarrow s}(\mathbf{k}_2) \left(\frac{\partial}{\partial \mathbf{r}_c} c_{\downarrow}(-\mathbf{k}_2) \right) - v_{\uparrow s}(\mathbf{k}_2) \left(\frac{\partial}{\partial \mathbf{r}_c} c_{\uparrow}(-\mathbf{k}_2) \right) \right] | G \rangle. \tag{B4}
 \end{aligned}$$

Here L_1 can be expressed in terms of the phase of the envelope function $w_s(\mathbf{k}, t)$ at the wave-packet center \mathbf{k}_c , i.e., $\theta_w(\mathbf{k}_c, t)$,

$$\begin{aligned} L_1 &= \int_{\mathbf{k}} |w_s(\mathbf{k}, t)|^2 \left(\frac{\partial}{\partial t} \theta_w(\mathbf{k}, t) + \frac{d\mathbf{r}_c}{dt} \cdot \frac{\partial}{\partial \mathbf{r}_c} \theta_w(\mathbf{k}, t) \right) \\ &= \frac{\partial}{\partial t} \theta_w(\mathbf{k}_c, t) + \frac{d\mathbf{r}_c}{dt} \cdot \frac{\partial}{\partial \mathbf{r}_c} \theta_w(\mathbf{k}_c, t). \end{aligned} \quad (\text{B5})$$

Using the expression for the wave-packet center \mathbf{r}_c in Eq. (A3), one can rewrite this equation as

$$\begin{aligned} L_1 &= \frac{d}{dt} \theta_w(\mathbf{k}_c, t) - \frac{d\mathbf{k}_c}{dt} \cdot \frac{\partial}{\partial \mathbf{k}_c} \theta_w(\mathbf{k}_c, t) \\ &= \frac{d}{dt} \theta_w(\mathbf{k}_c, t) - \dot{\mathbf{k}}_c \cdot (\mathbf{r}_c - \mathcal{A}_{ks}). \end{aligned} \quad (\text{B6})$$

Converting the electron operator c_σ into the quasiparticle operator γ_s in L_2 , we obtain

$$\begin{aligned} L_2 &= i \frac{d\mathbf{r}_c}{dt} \cdot \int_{\mathbf{k}_1, \mathbf{k}_2} w_s^*(\mathbf{k}_1, t) w_s(\mathbf{k}_2, t) \langle G | \gamma_s(\mathbf{k}_1) \left[\begin{array}{l} \left(\frac{\partial}{\partial \mathbf{r}_c} u_{\uparrow s}(\mathbf{k}_2) \right) \sum_{s'} (u_{\uparrow s'}^*(\mathbf{k}_2) \gamma_{s'}^\dagger(\mathbf{k}_2) - v_{\uparrow s'}(-\mathbf{k}_2) \gamma_{s'}(-\mathbf{k}_2)) \\ + \left(\frac{\partial}{\partial \mathbf{r}_c} u_{\downarrow s}(\mathbf{k}_2) \right) \sum_{s'} (u_{\downarrow s'}^*(\mathbf{k}_2) \gamma_{s'}^\dagger(\mathbf{k}_2) + v_{\downarrow s'}(-\mathbf{k}_2) \gamma_{s'}(-\mathbf{k}_2)) \\ + \left(\frac{\partial}{\partial \mathbf{r}_c} v_{\downarrow s}(\mathbf{k}_2) \right) \sum_{s'} (v_{\downarrow s'}^*(\mathbf{k}_2) \gamma_{s'}^\dagger(\mathbf{k}_2) + u_{\downarrow s'}(-\mathbf{k}_2) \gamma_{s'}(-\mathbf{k}_2)) \\ + \left(\frac{\partial}{\partial \mathbf{r}_c} v_{\uparrow s}(\mathbf{k}_2) \right) \sum_{s'} (v_{\uparrow s'}^*(\mathbf{k}_2) \gamma_{s'}^\dagger(\mathbf{k}_2) - u_{\uparrow s'}(-\mathbf{k}_2) \gamma_{s'}(-\mathbf{k}_2)) \end{array} \right] |G\rangle \\ &= i \frac{d\mathbf{r}_c}{dt} \cdot \int_{\mathbf{k}} |w_s(\mathbf{k}, t)|^2 \sum_{\sigma} \left(u_{\sigma s}^*(\mathbf{k}) \frac{\partial}{\partial \mathbf{r}_c} u_{\sigma s}(\mathbf{k}) + v_{\sigma s}^*(\mathbf{k}) \frac{\partial}{\partial \mathbf{r}_c} v_{\sigma s}(\mathbf{k}) \right) \\ &= \dot{\mathbf{r}}_c \cdot \mathcal{A}_{rs}. \end{aligned} \quad (\text{B7})$$

For the evaluation of L_3 , note that

$$\begin{aligned} \frac{d\mathbf{r}_c}{dt} \cdot \frac{\partial}{\partial \mathbf{r}_c} c_\sigma(\pm \mathbf{k}) &= \frac{d\mathbf{r}_c}{dt} \cdot \frac{\partial}{\partial \mathbf{r}_c} \left(\int d^2 \mathbf{r} e^{-i(\pm \mathbf{k} + \mathbf{A}(\mathbf{r}_c)) \cdot \mathbf{r}} c_\sigma(\mathbf{r}) \right) \\ &= -i \frac{d\mathbf{r}_c}{dt} \cdot \int_{\mathbf{r}} \frac{\partial \mathbf{A}(\mathbf{r}_c) \cdot \mathbf{r}}{\partial \mathbf{r}_c} e^{-i(\pm \mathbf{k} + \mathbf{A}(\mathbf{r}_c)) \cdot \mathbf{r}} c_\sigma(\mathbf{r}) \\ &= \frac{d\mathbf{A}(\mathbf{r}_c)}{dt} \cdot \int d^2 \mathbf{r} \left(\pm \frac{\partial}{\partial \mathbf{k}} e^{-i(\pm \mathbf{k} + \mathbf{A}(\mathbf{r}_c)) \cdot \mathbf{r}} \right) c_\sigma(\mathbf{r}) \\ &= \pm \frac{d\mathbf{A}(\mathbf{r}_c)}{dt} \cdot \frac{\partial}{\partial \mathbf{k}} c_\sigma(\pm \mathbf{k}), \end{aligned} \quad (\text{B8})$$

which leads to

$$\begin{aligned} L_3 &= i \frac{d}{dt} \mathbf{A}(\mathbf{r}_c) \cdot \int_{\mathbf{k}_1, \mathbf{k}_2} w_s^*(\mathbf{k}_1, t) w_s(\mathbf{k}_2, t) \\ &\quad \times \langle \Omega | \gamma_s(\mathbf{k}_1) \left[u_{\uparrow s}(\mathbf{k}_2) \left(\frac{\partial}{\partial \mathbf{k}_2} c_{\uparrow}^\dagger(\mathbf{k}_2) \right) + u_{\downarrow s}(\mathbf{k}_2) \left(\frac{\partial}{\partial \mathbf{k}_2} c_{\downarrow}^\dagger(\mathbf{k}_2) \right) - v_{\downarrow s}(\mathbf{k}_2) \left(\frac{\partial}{\partial \mathbf{k}_2} c_{\downarrow}(-\mathbf{k}_2) \right) + v_{\uparrow s}(\mathbf{k}_2) \left(\frac{\partial}{\partial \mathbf{k}_2} c_{\uparrow}(-\mathbf{k}_2) \right) \right] | \Omega \rangle \\ &= -i \frac{d}{dt} \mathbf{A}(\mathbf{r}_c) \cdot \int_{\mathbf{k}} w_s^*(\mathbf{k}, t) (\partial_{\mathbf{k}} w_s(\mathbf{k}, t)) (|u_{\sigma s}(\mathbf{k})|^2 - |v_{\sigma s}(\mathbf{k})|^2) \\ &\quad - i \frac{d}{dt} \mathbf{A}(\mathbf{r}_c) \cdot \int_{\mathbf{k}} |w_s(\mathbf{k}, t)|^2 (u_{\sigma s}^*(\mathbf{k}) \partial_{\mathbf{k}} u_{\sigma s}(\mathbf{k}) - v_{\sigma s}^*(\mathbf{k}) \partial_{\mathbf{k}} v_{\sigma s}(\mathbf{k})). \end{aligned} \quad (\text{B9})$$

Comparing this equation with the expression for the electric dipole moment \mathbf{d} (see Eqs. (A10) and (A11)), it is easy to see that L_3 can be expressed as

$$L_3 = -\dot{\mathbf{A}}(\mathbf{r}_c) \cdot [\rho_{0s}(\mathbf{k}_c) \mathbf{r}_c + \mathbf{d}]. \quad (\text{B10})$$

Combining everything, we obtain

$$L = -E_s(k_c) - \dot{\mathbf{k}}_c \cdot (\mathbf{r}_c - \mathcal{A}_{ks}) + \dot{\mathbf{r}}_c \cdot \mathcal{A}_{rs} - \dot{\mathbf{A}}(\mathbf{r}_c) \cdot [\rho_{0s}(\mathbf{k}_c) \mathbf{r}_c + \mathbf{d}]. \quad (\text{B11})$$

Here we have dropped terms, which can be expressed as total time derivatives and as a result do not enter the equation of motion. Using $\mathbf{A}(\mathbf{r}_c) = \frac{1}{2}\mathbf{B} \times \mathbf{r}_c$, we find that the Lagrangian can be rewritten as Eq. (13).

APPENDIX C: EQUATION OF MOTION

In this Appendix, we derive the explicit expression for the equation of motion of the quasiparticle wave-packet dynamics in terms of the coherence factors. Inserting the expression for the Lagrangian in Eq. (13) into the Euler-Lagrange equation

$$\frac{\partial L}{\partial r_c^i} = \frac{d}{dt} \frac{\partial L}{\partial \dot{r}_c^i}, \quad \frac{\partial L}{\partial k_c^i} = \frac{d}{dt} \frac{\partial L}{\partial \dot{k}_c^i}, \quad i = x, y, \quad (\text{C1})$$

one can derive the equation of motion for the wave-packet center:

$$\begin{aligned} \dot{k}_c^i &= -\partial_{r_c^i} E_s(k_c) + \Omega_{rks}^{ij} \dot{k}_c^j + \Omega_{rrs}^{ij} \dot{r}_c^j, \\ \dot{r}_c^i &= \partial_{k_c^i} E_s(k_c) - \Omega_{kks}^{ij} \dot{k}_c^j - \Omega_{krs}^{ij} \dot{r}_c^j. \end{aligned} \quad (\text{C2})$$

Here we have employed the notation that repeated indices implies summation. Note that the Berry curvatures Ω are defined as derivatives of the Berry connections \mathcal{A}_{ks} and \mathcal{A}_{rs} :

$$\begin{aligned} \Omega_{kks}^{ij} &\equiv \partial_{k_c^i} \mathcal{A}_{ks}^j - \partial_{k_c^j} \mathcal{A}_{ks}^i, \quad \Omega_{rrs}^{ij} \equiv \partial_{r_c^i} \mathcal{A}_{rs}^j - \partial_{r_c^j} \mathcal{A}_{rs}^i, \\ \Omega_{rks}^{ij} &\equiv -\Omega_{krs}^{ji} \equiv \partial_{r_c^i} \mathcal{A}_{ks}^j - \partial_{k_c^j} \mathcal{A}_{rs}^i. \end{aligned} \quad (\text{C3})$$

Equation (C2) can be rewritten in a vector form:

$$\begin{aligned} \dot{\mathbf{k}}_c &= -\nabla_{\mathbf{r}_c} E_s(k_c) + \dot{\mathbf{r}}_c \times \mathbf{\Omega}_{rs} + \nabla_{\mathbf{r}_c} (\dot{\mathbf{k}}_c \cdot \mathcal{A}_{ks}) - (\dot{\mathbf{k}}_c \cdot \nabla_{\mathbf{k}_c}) \mathcal{A}_{rs}, \\ \dot{\mathbf{r}}_c &= \nabla_{\mathbf{k}_c} E_s(k_c) - \dot{\mathbf{k}}_c \times \mathbf{\Omega}_{ks} - \nabla_{\mathbf{k}_c} (\dot{\mathbf{r}}_c \cdot \mathcal{A}_{rs}) + (\dot{\mathbf{r}}_c \cdot \nabla_{\mathbf{r}_c}) \mathcal{A}_{rs}. \end{aligned} \quad (\text{C4})$$

Here the vector forms of the Berry curvatures $\mathbf{\Omega}_{rs}$ and $\mathbf{\Omega}_{ks}$ are defined as

$$\mathbf{\Omega}_{ks} = \nabla_{\mathbf{k}_c} \times \mathcal{A}_{ks}, \quad \mathbf{\Omega}_{rs} = \nabla_{\mathbf{r}_c} \times \mathcal{A}_{rs}, \quad (\text{C5})$$

and they are related to their tensor counterparts Ω_{rrs} and Ω_{kks} by:

$$\mathbf{\Omega}_{rs/ks}^l = \frac{1}{2} \epsilon_{lij} \Omega_{rrs/kks}^{ij}, \quad \Omega_{rrs/kks}^{ij} = \epsilon_{ijl} \mathbf{\Omega}_{rs/ks}^l, \quad (\text{C6})$$

with ϵ_{ijl} being the Levi-Civita symbol. Note that in the present paper, we consider a 2D system, and therefore only the z component of the vector Berry curvature $\mathbf{\Omega}$ is nonvanishing.

Using the expressions for the Berry connections \mathcal{A}_{ks} and \mathcal{A}_{rs} , we obtain

$$\begin{aligned} \mathbf{\Omega}_{ks} &= -\frac{1}{2} \nabla_{\mathbf{k}_c} \rho_{0s}(\mathbf{k}_c) \times \nabla_{\mathbf{k}_c} \chi + \frac{1}{2} \nabla_{\mathbf{k}_c} \rho_{1s}(\mathbf{k}_c) \times \nabla_{\mathbf{k}_c} \phi_{\mathbf{k}_c}, \\ \mathbf{\Omega}_{rs} &= -\nabla_{\mathbf{r}_c} \rho_{0s}(\mathbf{k}_c) \times (\nabla_{\mathbf{r}_c} \chi / 2 - \mathbf{A}(\mathbf{r}_c)) + \rho_{0s}(\mathbf{k}_c) \mathbf{B} + \frac{1}{2} \nabla_{\mathbf{r}_c} \times (\mathbf{B} \times \mathbf{d}) + \frac{1}{2} \nabla_{\mathbf{r}_c} \rho_{1s}(\mathbf{k}_c) \times \nabla_{\mathbf{r}_c} \phi_{\mathbf{k}_c}. \end{aligned} \quad (\text{C7})$$

The tensor-form of the phase-space Berry curvature Ω_{rk} is given by,

$$\Omega_{rks}^{ij} = -\frac{1}{2} (\partial_{r_c^i} \rho_{0s}(\mathbf{k}_c) \partial_{k_c^j} \chi - \partial_{k_c^i} \rho_{0s}(\mathbf{k}_c) \partial_{r_c^j} \chi) + \frac{1}{2} (\partial_{r_c^i} \rho_{1s}(\mathbf{k}_c) \partial_{k_c^j} \phi_{\mathbf{k}_c} - \partial_{k_c^i} \rho_{1s}(\mathbf{k}_c) \partial_{r_c^j} \phi_{\mathbf{k}_c}) - \partial_{k_c^i} \rho_{0s}(\mathbf{k}_c) \mathbf{A}^i(\mathbf{r}_c) - \frac{1}{2} \partial_{k_c^i} (\mathbf{B} \times \mathbf{d})^i. \quad (\text{C8})$$

Inserting Eq. (C7) into Eq. (C4) leads to the following form of the equation of motion:

$$\begin{aligned} \dot{\mathbf{k}}_c &= -\nabla_{\mathbf{r}_c} E_s(k_c) + \dot{\mathbf{r}}_c \times \left[-\nabla_{\mathbf{r}_c} \rho_{0s}(\mathbf{k}_c) \times \left(\frac{1}{2} \nabla_{\mathbf{r}_c} \chi - \mathbf{A}(\mathbf{r}_c) \right) + \rho_{0s}(\mathbf{k}_c) \mathbf{B} + \frac{1}{2} \nabla_{\mathbf{r}_c} \times (\mathbf{B} \times \mathbf{d}) + \frac{1}{2} \nabla_{\mathbf{r}_c} \rho_{1s}(\mathbf{k}_c) \times \nabla_{\mathbf{r}_c} \phi_{\mathbf{k}_c} \right] \\ &\quad - \frac{1}{2} \nabla_{\mathbf{r}_c} [\dot{\mathbf{k}}_c \cdot (\rho_{0s}(\mathbf{k}_c) \nabla_{\mathbf{k}_c} \chi - \rho_{1s}(\mathbf{k}_c) \nabla_{\mathbf{k}_c} \phi_{\mathbf{k}_c})] + (\dot{\mathbf{k}}_c \cdot \nabla_{\mathbf{k}_c}) [\rho_{0s}(\mathbf{k}_c) \left(\frac{1}{2} \nabla_{\mathbf{r}_c} \chi - \mathbf{A}(\mathbf{r}_c) \right) - \frac{1}{2} \mathbf{B} \times \mathbf{d} - \frac{1}{2} \rho_{1s}(\mathbf{k}_c) \nabla_{\mathbf{r}_c} \phi_{\mathbf{k}_c}], \\ \dot{\mathbf{r}}_c &= \nabla_{\mathbf{k}_c} E_s(k_c) - \dot{\mathbf{k}}_c \times \left(-\frac{1}{2} \nabla_{\mathbf{k}_c} \rho_{0s}(\mathbf{k}_c) \times \nabla_{\mathbf{k}_c} \chi + \frac{1}{2} \nabla_{\mathbf{k}_c} \rho_{1s}(\mathbf{k}_c) \times \nabla_{\mathbf{k}_c} \phi_{\mathbf{k}_c} \right) \\ &\quad + \nabla_{\mathbf{k}_c} \{ \dot{\mathbf{r}}_c \cdot [\rho_{0s}(\mathbf{k}_c) \left(\frac{1}{2} \nabla_{\mathbf{r}_c} \chi - \mathbf{A}(\mathbf{r}_c) \right) - \frac{1}{2} \mathbf{B} \times \mathbf{d} - \frac{1}{2} \rho_{1s}(\mathbf{k}_c) \nabla_{\mathbf{r}_c} \phi_{\mathbf{k}_c}] \} - \frac{1}{2} (\dot{\mathbf{r}}_c \cdot \nabla_{\mathbf{r}_c}) (\rho_{0s}(\mathbf{k}_c) \nabla_{\mathbf{k}_c} \chi - \rho_{1s}(\mathbf{k}_c) \nabla_{\mathbf{k}_c} \phi_{\mathbf{k}_c}), \end{aligned} \quad (\text{C9})$$

where the dependence of ρ_{as} on the coherence factors is given in Eqs. (15) and (19).

APPENDIX D: BERRY CURVATURE CORRECTION TO THE PHASE-SPACE DENSITY OF STATES

As mentioned in the main text, the equation of motion Eq. (C2) exhibits a noncanonical structure due to the presence of the Berry curvatures, which leads to the breakdown of the conservation of the phase-space volume. In particular, the phase-space volume element $\Delta V = \Delta\mathbf{k}\Delta\mathbf{r}$ is no longer constant in time and instead evolves according to [27]

$$\frac{1}{\Delta V} \frac{d\Delta V}{dt} = \nabla_{\mathbf{r}} \cdot \dot{\mathbf{r}} + \nabla_{\mathbf{k}} \cdot \dot{\mathbf{k}}. \quad (\text{D1})$$

One therefore needs to introduce a modified phase-space density of states $D(\mathbf{r}, \mathbf{k})$ such that the number of states in volume element ΔV , i.e., $D(\mathbf{r}, \mathbf{k})\Delta V$, remains constant over time. This Appendix provides the derivation of the correction to the phase-space density of states induced by the Berry curvatures for the current model.

In terms of the Berry curvatures, up to an inessential coefficient, the modified phase-space density of states $D(\mathbf{r}, \mathbf{k})$ acquires a form [29,57]

$$D = \sqrt{\det \begin{bmatrix} \Omega_{rrs} & \Omega_{rks} - I \\ \Omega_{krs} + I & \Omega_{kks} \end{bmatrix}}. \quad (\text{D2})$$

Since the external perturbation is assumed to be slowly varying in real space, one can perform an expansion in terms of the spatial gradient and keep only the leading-order terms [34]. The Berry curvature correction to the phase-space density of states $\delta D \equiv D - 1$ therefore can be approximated by

$$\begin{aligned} \delta D(\mathbf{r}, \mathbf{k}) &= \text{Tr} \Omega_{krs} - \Omega_{rs} \cdot \Omega_{ks} \\ &= -\nabla_{\mathbf{k}} \rho_{0s} \cdot \mathbf{p}_s - \frac{1}{2} \mathbf{B} \cdot (\nabla_{\mathbf{k}} \times \mathbf{d}) + \frac{1}{2} \nabla_{\mathbf{r}} \rho_{0s} \cdot \nabla_{\mathbf{k}} \chi + \frac{1}{2} \nabla_{\mathbf{k}} \rho_{1s} \cdot \nabla_{\mathbf{r}} \phi_{\mathbf{k}} - \frac{1}{2} \nabla_{\mathbf{r}} \rho_{1s} \cdot \nabla_{\mathbf{k}} \phi_{\mathbf{k}} \\ &\quad - \frac{1}{2} (\nabla_{\mathbf{k}} \rho_{0s} \times \nabla_{\mathbf{k}} \chi - \nabla_{\mathbf{k}} \rho_{1s} \times \nabla_{\mathbf{k}} \phi_{\mathbf{k}}) \cdot (\nabla_{\mathbf{r}} \rho_{0s}(\mathbf{k}) \times \mathbf{p}_s - \rho_{0s} \mathbf{B} - \frac{1}{2} \nabla_{\mathbf{r}} \times (\mathbf{B} \times \mathbf{d}) - \frac{1}{2} \nabla_{\mathbf{r}} \rho_{1s}(\mathbf{k}) \times \nabla_{\mathbf{r}} \phi_{\mathbf{k}}), \end{aligned} \quad (\text{D3})$$

where in the second step we have inserted the explicit expressions for the Berry curvatures. \mathbf{p}_s denotes the supercurrent $\mathbf{p}_s \equiv \frac{1}{2} \nabla_{\mathbf{r}} \chi - \mathbf{A}$.

We now separate δD into three different components: the external magnetic field \mathbf{B} -dependent part δD_1 , the supercurrent \mathbf{p}_s -dependent part δD_2 , and the remaining part δD_3 :

$$\begin{aligned} \delta D_1(\mathbf{r}, \mathbf{k}) &= -\frac{1}{2} \mathbf{B} \cdot (\nabla_{\mathbf{k}} \times \mathbf{d}) + \frac{1}{2} (\nabla_{\mathbf{k}} \rho_{0s} \times \nabla_{\mathbf{k}} \chi - \nabla_{\mathbf{k}} \rho_{1s} \times \nabla_{\mathbf{k}} \phi_{\mathbf{k}}) \cdot [\rho_{0s} \mathbf{B} + \frac{1}{2} \nabla_{\mathbf{r}} \times (\mathbf{B} \times \mathbf{d})], \\ \delta D_2(\mathbf{r}, \mathbf{k}) &= -\nabla_{\mathbf{k}} \rho_{0s} \cdot \mathbf{p}_s - \frac{1}{2} (\nabla_{\mathbf{k}} \rho_{0s} \times \nabla_{\mathbf{k}} \chi - \nabla_{\mathbf{k}} \rho_{1s} \times \nabla_{\mathbf{k}} \phi_{\mathbf{k}}) \cdot (\nabla_{\mathbf{r}} \rho_{0s} \times \mathbf{p}_s), \\ \delta D_3(\mathbf{r}, \mathbf{k}) &= \frac{1}{2} (\nabla_{\mathbf{r}} \rho_{0s} \cdot \nabla_{\mathbf{k}} \chi + \nabla_{\mathbf{k}} \rho_{1s} \cdot \nabla_{\mathbf{r}} \phi_{\mathbf{k}} - \nabla_{\mathbf{r}} \rho_{1s} \cdot \nabla_{\mathbf{k}} \phi_{\mathbf{k}}) + \frac{1}{4} (\nabla_{\mathbf{k}} \rho_{0s} \times \nabla_{\mathbf{k}} \chi - \nabla_{\mathbf{k}} \rho_{1s} \times \nabla_{\mathbf{k}} \phi_{\mathbf{k}}) \cdot (\nabla_{\mathbf{r}} \rho_{1s} \times \nabla_{\mathbf{r}} \phi_{\mathbf{k}}). \end{aligned} \quad (\text{D4})$$

Dropping the higher-order terms in the spatial gradient $\nabla_{\mathbf{r}}$ in the equation above, we find $\delta D_3 = 0$ and $\delta D_2 = -\nabla_{\mathbf{k}} \rho_{0s} \cdot \mathbf{p}_s$, which is not considered in this paper. We focus instead on the component $\delta D_1(\mathbf{r}, \mathbf{k})$, which evaluates to

$$\begin{aligned} \delta D_1(\mathbf{r}, \mathbf{k}) &= -\frac{1}{2} \mathbf{B} \cdot (\nabla_{\mathbf{k}} \times \mathbf{d}) + \frac{1}{2} \rho_{0s} (\nabla_{\mathbf{k}} \rho_{0s} \times \nabla_{\mathbf{k}} \chi - \nabla_{\mathbf{k}} \rho_{1s} \times \nabla_{\mathbf{k}} \phi_{\mathbf{k}}) \cdot \mathbf{B} \\ &= -\frac{1}{4} \mathbf{B} \cdot [(\nabla_{\mathbf{k}} \rho_{2s} + \rho_{0s} \nabla_{\mathbf{k}} \rho_{1s} - \rho_{1s} \nabla_{\mathbf{k}} \rho_{0s}) \times \nabla_{\mathbf{k}} \phi_{\mathbf{k}}]. \end{aligned} \quad (\text{D5})$$

Here in the second equality, we have inserted the expression for \mathbf{d} in Eq. (A11). Note that this expression reduces to Eq. (23) for s -wave pairing $\chi = 0$.

[1] N. Read and D. Green, Paired states of fermions in two dimensions with breaking of parity and time-reversal symmetries and the fractional quantum Hall effect, *Phys. Rev. B* **61**, 10267 (2000).

[2] A. Y. Kitaev, Unpaired Majorana fermions in quantum wires, *Phys. Usp.* **44**, 131 (2001).

[3] L. Jiao, S. Howard, S. Ran, Z. Wang, J. O. Rodriguez, M. Sigrist, Z. Wang, N. P. Butch, and V. Madhavan, Chiral superconductivity in heavy-fermion metal UTe_2 , *Nature (London)* **579**, 523 (2020).

[4] E. Khalaf, Higher-order topological insulators and superconductors protected by inversion symmetry, *Phys. Rev. B* **97**, 205136 (2018).

[5] R.-X. Zhang, W. S. Cole, X. Wu, and S. Das Sarma, Higher-order topology and nodal topological superconductivity in $\text{Fe}(\text{Se},\text{Te})$ heterostructures, *Phys. Rev. Lett.* **123**, 167001 (2019).

[6] Y.-T. Hsu, W. S. Cole, R.-X. Zhang, and J. D. Sau, Inversion-protected higher-order topological superconductivity in monolayer WTe_2 , *Phys. Rev. Lett.* **125**, 097001 (2020).

[7] S.-J. Huang, K. Park, and Y.-T. Hsu, Hybrid-order topological superconductivity in a topological metal $1t'\text{-MoTe}_2$, *npj Quantum Mater.* **9**, 21 (2024).

[8] B. E. Feldman, M. T. Randeria, J. Li, S. Jeon, Y. Xie, Z. Wang, I. K. Drozdov, B. Andrei Bernevig, and A. Yazdani, High-resolution studies of the Majorana atomic chain platform, *Nat. Phys.* **13**, 286 (2017).

[9] G. C. Ménard, S. Guissart, C. Brun, R. T. Leriche, M. Trif, F. Debontridder, D. Demaille, D. Roditchev, P. Simon, and

T. Cren, Two-dimensional topological superconductivity in Pb/Co/Si(111), *Nat. Commun.* **8**, 2040 (2017).

[10] P. Zhang, K. Yaji, T. Hashimoto, Y. Ota, T. Kondo, K. Okazaki, Z. Wang, J. Wen, G. D. Gu, H. Ding, and S. Shin, Observation of topological superconductivity on the surface of an iron-based superconductor, *Science* **360**, 182 (2018).

[11] D. Wang, L. Kong, P. Fan, H. Chen, S. Zhu, W. Liu, L. Cao, Y. Sun, S. Du, J. Schneeloch, R. Zhong, G. Gu, L. Fu, H. Ding, and H.-J. Gao, Evidence for Majorana bound states in an iron-based superconductor, *Science* **362**, 333 (2018).

[12] B. Jäck, Y. Xie, J. Li, S. Jeon, B. A. Bernevig, and A. Yazdani, Observation of a Majorana zero mode in a topologically protected edge channel, *Science* **364**, 1255 (2019).

[13] A. Palacio-Morales, E. Mascot, S. Cocklin, H. Kim, S. Rachel, D. K. Morr, and R. Wiesendanger, Atomic-scale interface engineering of Majorana edge modes in a 2D magnet-superconductor hybrid system, *Sci. Adv.* **5**, eaav6600 (2019).

[14] S. Manna, P. Wei, Y. Xie, K. T. Law, P. A. Lee, and J. S. Moodera, Signature of a pair of Majorana zero modes in superconducting gold surface states, *Proc. Natl. Acad. Sci. USA* **117**, 8775 (2020).

[15] S. Kezilebieke, M. N. Huda, V. Vaňo, M. Aapro, S. C. Ganguli, O. J. Silveira, S. Głodzik, A. S. Foster, T. Ojanen, and P. Liljeroth, Topological superconductivity in a van der Waals heterostructure, *Nature (London)* **588**, 424 (2020).

[16] Z. Wang, J. O. Rodriguez, L. Jiao, S. Howard, M. Graham, G. D. Gu, T. L. Hughes, D. K. Morr, and V. Madhavan, Evidence for dispersing 1D Majorana channels in an iron-based superconductor, *Science* **367**, 104 (2020).

[17] B. Jäck, Y. Xie, and A. Yazdani, Detecting and distinguishing Majorana zero modes with the scanning tunnelling microscope, *Nat. Rev. Phys.* **3**, 541 (2021).

[18] P. Yu, J. Chen, M. Gomanko, G. Badawy, E. P. A. M. Bakkers, K. Zuo, V. Mourik, and S. M. Frolov, Non-Majorana states yield nearly quantized conductance in proximitized nanowires, *Nat. Phys.* **17**, 482 (2021).

[19] Y. Peng, F. Pientka, Y. Vinkler-Aviv, L. I. Glazman, and F. von Oppen, Robust Majorana conductance peaks for a superconducting lead, *Phys. Rev. Lett.* **115**, 266804 (2015).

[20] J. Li, S. Jeon, Y. Xie, A. Yazdani, and B. A. Bernevig, Majorana spin in magnetic atomic chain systems, *Phys. Rev. B* **97**, 125119 (2018).

[21] H. Zhang, C.-X. Liu, S. Gazibegovic, D. Xu, J. A. Logan, G. Wang, N. van Loo, J. D. S. Bommer, M. W. A. de Moor, D. Car, R. L. M. Op het Veld, P. J. van Veldhoven, S. Koelling, M. A. Verheijen, M. Pendharkar, D. J. Pennachio, B. Shojaei, J. S. Lee, C. J. Palmstrøm, E. P. A. M. Bakkers *et al.*, Retracted article: Quantized Majorana conductance, *Nature (London)* **556**, 74 (2018).

[22] H. Pan and S. Das Sarma, Physical mechanisms for zero-bias conductance peaks in Majorana nanowires, *Phys. Rev. Res.* **2**, 013377 (2020).

[23] S. M. Frolov, M. J. Manfra, and J. D. Sau, Topological superconductivity in hybrid devices, *Nat. Phys.* **16**, 718 (2020).

[24] H. Pan, W. S. Cole, J. D. Sau, and S. Das Sarma, Generic quantized zero-bias conductance peaks in superconductor-semiconductor hybrid structures, *Phys. Rev. B* **101**, 024506 (2020).

[25] M. Valentini, F. Peñaranda, A. Hofmann, M. Brauns, R. Hauschild, P. Krogstrup, P. San-Jose, E. Prada, R. Aguado, and G. Katsaros, Nontopological zero-bias peaks in full-shell nanowires induced by flux-tunable Andreev states, *Science* **373**, 82 (2021).

[26] G. Sundaram and Q. Niu, Wave-packet dynamics in slowly perturbed crystals: Gradient corrections and Berry-phase effects, *Phys. Rev. B* **59**, 14915 (1999).

[27] D. Xiao, J. Shi, and Q. Niu, Berry phase correction to electron density of states in solids, *Phys. Rev. Lett.* **95**, 137204 (2005).

[28] R. Shindou and K.-I. Imura, Noncommutative geometry and non-Abelian Berry phase in the wave-packet dynamics of Bloch electrons, *Nucl. Phys. B* **720**, 399 (2005).

[29] D. Xiao, M.-C. Chang, and Q. Niu, Berry phase effects on electronic properties, *Rev. Mod. Phys.* **82**, 1959 (2010).

[30] Y. Gao, S. A. Yang, and Q. Niu, Geometrical effects in orbital magnetic susceptibility, *Phys. Rev. B* **91**, 214405 (2015).

[31] A. Julku, S. Peotta, T. I. Vanhala, D.-H. Kim, and P. Törmä, Geometric origin of superfluidity in the Lieb-Lattice flat band, *Phys. Rev. Lett.* **117**, 045303 (2016).

[32] L. Liang, S. Peotta, A. Harju, and P. Törmä, Wave-packet dynamics of Bogoliubov quasiparticles: Quantum metric effects, *Phys. Rev. B* **96**, 064511 (2017).

[33] L. Liang, T. I. Vanhala, S. Peotta, T. Siro, A. Harju, and P. Törmä, Band geometry, Berry curvature, and superfluid weight, *Phys. Rev. B* **95**, 024515 (2017).

[34] Z. Wang, L. Dong, C. Xiao, and Q. Niu, Berry curvature effects on quasiparticle dynamics in superconductors, *Phys. Rev. Lett.* **126**, 187001 (2021).

[35] E. Rossi, Quantum metric and correlated states in two-dimensional systems, *Curr. Opin. Solid State Mater. Sci.* **25**, 100952 (2021).

[36] J. Ahn and N. Nagaosa, Superconductivity-induced spectral weight transfer due to quantum geometry, *Phys. Rev. B* **104**, L100501 (2021).

[37] J. Yu, C. J. Ciccarino, R. Bianco, I. Errea, P. Narang, and B. A. Bernevig, Non-trivial quantum geometry and the strength of electronphonon coupling, *Nat. Phys.* **20**, 1262 (2024).

[38] L. Fu and C. L. Kane, Superconducting proximity effect and Majorana fermions at the surface of a topological insulator, *Phys. Rev. Lett.* **100**, 096407 (2008).

[39] P. A. Lee, [arXiv:0907.2681](https://arxiv.org/abs/0907.2681).

[40] J. D. Sau, R. M. Lutchyn, S. Tewari, and S. Das Sarma, Generic new platform for topological quantum computation using semiconductor heterostructures, *Phys. Rev. Lett.* **104**, 040502 (2010).

[41] J. D. Sau, S. Tewari, R. M. Lutchyn, T. D. Stanescu, and S. Das Sarma, Non-Abelian quantum order in spin-orbit-coupled semiconductors: Search for topological Majorana particles in solid-state systems, *Phys. Rev. B* **82**, 214509 (2010).

[42] M. Duckheim and P. W. Brouwer, Andreev reflection from non-centrosymmetric superconductors and Majorana bound-state generation in half-metallic ferromagnets, *Phys. Rev. B* **83**, 054513 (2011).

[43] S. B. Chung, H.-J. Zhang, X.-L. Qi, and S.-C. Zhang, Topological superconducting phase and Majorana fermions in half-metal/superconductor heterostructures, *Phys. Rev. B* **84**, 060510(R) (2011).

[44] A. C. Potter and P. A. Lee, Topological superconductivity and Majorana fermions in metallic surface states, *Phys. Rev. B* **85**, 094516 (2012).

[45] J. Röntynen and T. Ojanen, Topological superconductivity and high chern numbers in 2D ferromagnetic shiba lattices, *Phys. Rev. Lett.* **114**, 236803 (2015).

[46] J. Li, T. Neupert, Z. Wang, A. H. MacDonald, A. Yazdani, and B. A. Bernevig, Two-dimensional chiral topological superconductivity in Shiba lattices, *Nat. Commun.* **7**, 12297 (2016).

[47] Y.-T. Hsu, A. Vaezi, M. H. Fischer, and E.-A. Kim, Topological superconductivity in monolayer transition metal dichalcogenides, *Nat. Commun.* **8**, 14985 (2017).

[48] J. Wang, W. Powers, Z. Zhang, M. Smith, B. J. McIntosh, S. K. Bac, L. Riney, M. Zhukovskyi, T. Orlova, L. P. Rokhinson, Y.-T. Hsu, X. Liu, and B. A. Assaf, Observation of coexisting weak localization and superconducting fluctuations in strained $\text{Sn}_{1-x}\text{In}_x\text{Te}$ thin films, *Nano Lett.* **22**, 792 (2022).

[49] J. Jang, H. M. Yoo, L. N. Pfeiffer, K. W. West, K. W. Baldwin, and R. C. Ashoori, Full momentum- and energy-resolved spectral function of a 2D electronic system, *Science* **358**, 901 (2017).

[50] J. Huang, Z. Yue, A. Baydin, H. Zhu, H. Nojiri, J. Kono, Y. He, and M. Yi, Angle-resolved photoemission spectroscopy with an in situ tunable magnetic field, *Rev. Sci. Instrum.* **94**, 093902 (2023).

[51] L. Dong, C. Xiao, B. Xiong, and Q. Niu, Berry phase effects in dipole density and the Mott relation, *Phys. Rev. Lett.* **124**, 066601 (2020).

[52] S. A. Parameswaran, S. A. Kivelson, R. Shankar, S. L. Sondhi, and B. Z. Spivak, Microscopic model of quasiparticle wave packets in superfluids, superconductors, and paired Hall states, *Phys. Rev. Lett.* **109**, 237004 (2012).

[53] Here we keep $\partial_{\mathbf{k}}\chi$ for a general pairing symmetry, but later we will restrict ourselves to the case of *s* wave with $\partial_{\mathbf{k}}\chi = 0$ for the evaluation of BC correction to observables.

[54] D. Culcer, Y. Yao, and Q. Niu, Coherent wave-packet evolution in coupled bands, *Phys. Rev. B* **72**, 085110 (2005).

[55] The wave-packet average of an operator \hat{O} refers to $\langle W_s | \hat{O} | W_s \rangle - \langle G | \hat{O} | G \rangle$.

[56] L. Landau, E. Lifshitz, *Electrodynamics of Continuous Media* (Pergamon, New York, 1960).

[57] V. I. Arnold, *Mathematical Methods of Classical Mechanics* (Springer, New York, 1978).

[58] J. R. Schrieffer, *Theory of Superconductivity* (Perseus Books, Reading, 1983).

[59] The contribution from the penetration depth is expected to be negligible in the weak field regime, where the vortices are sparse compared to the beam size.